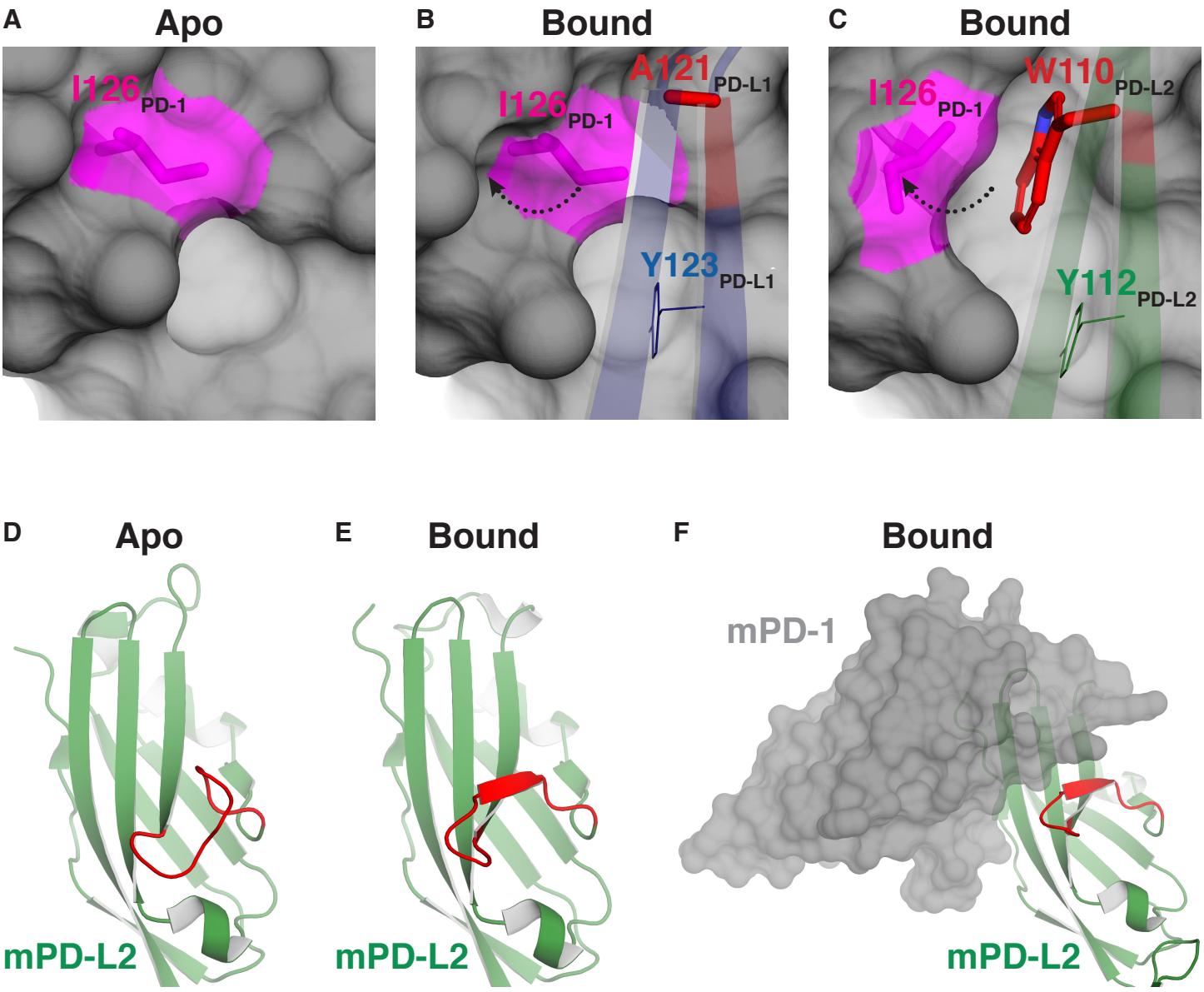

Figure S1. Unique structural features of PD-L2. (A-C) I126PD-1 rotates to accommodate W110PD-L2. The position of I126PD-1 (magenta) in the Apo state (PDB ID: 1NPU) (A), hPD-L1 bound state (PDB ID: 3BIK) (B), versus in the mPD-L2 bound state (PDB ID: 3BP5) (C). (D and E) Structures of the Apo (PDB ID: 3BOV) and PD-1 bound (PDB ID: 3BP5) states showing the reorientation of the C–D loop (red) into a "latch." (F) Positioning of the PD-L2 latch around a surface representation of the mPD-1 IgV domain (grey).

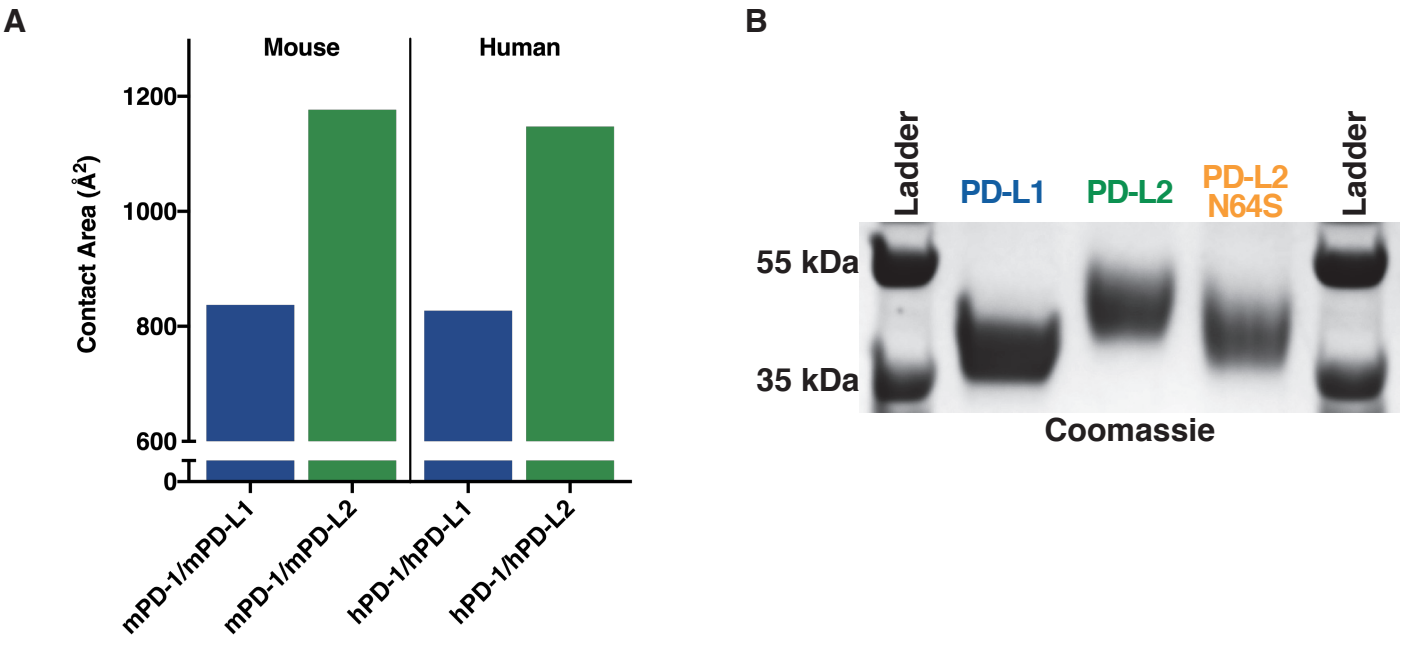

Figure S2. PD-L2 makes more contact with PD-1 and is glycosylated on N64. (A) Total buried surface areas of mPD-1/mPD-L1 (PDB ID: 3BIK), mPD-1/mPDL2 (PDB ID 3BP5), hPD-1/hPD-L1 (PDB ID: 4ZQK), and hPD-1/hPD-L2 (20) complexes calculated using Molsoft ICM (35). (B) The indicated PD-ligand ectodomains were expressed in HEK293 cells as secretory proteins, purified from conditioned medium and analyzed by SDS-PAGE (12% polyacrylamide gel). The increased electrophoretic mobility of the N64SPD-L2 substitution indicates N-linked glycosylation.

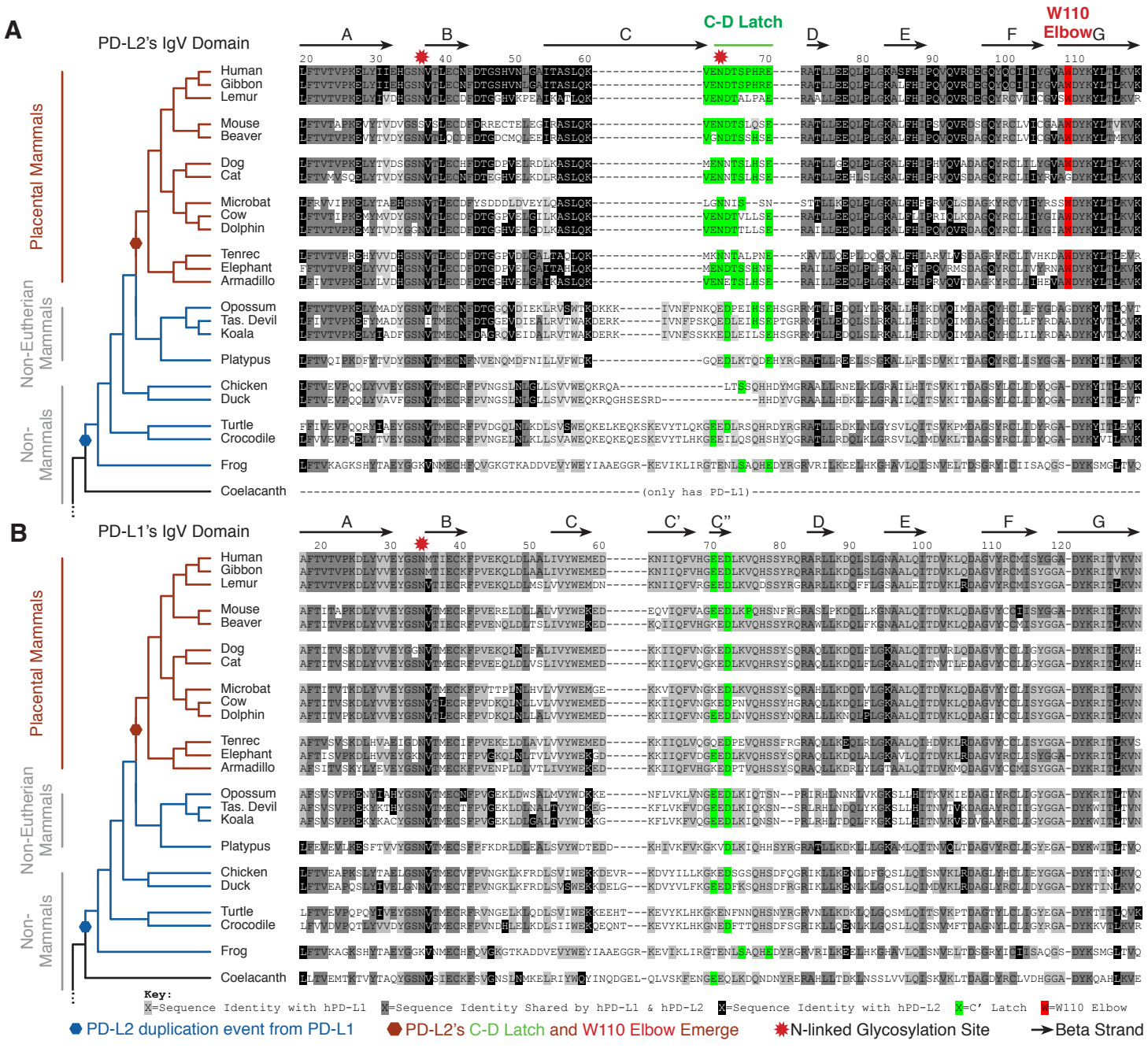
A
PD-L2's IgV Domain
C-D Latch
W110 Elbow
Placental Mammals
Non-Eutherian Mammals
Non-Mammals
Human
Gibbon
Lemur
Mouse
Beaver
Dog
Cat
Microbat
Cow
Dolphin
Tenrec
Elephant
Armadillo
Opossum
Tas. Devil
Koala
Platypus
Chicken
Duck
Turtle
Crocodile
Frog
Coelacanth
(only has PD-L1)
B
PD-L1's IgV Domain
Key:
X=Sequence Identity with hPD-L1
X=Sequence Identity Shared by hPD-L1 & hPD-L2
X=Sequence Identity with hPD-L2
X=C' Latch
X=W110 Elbow
PD-L2 duplication event from PD-L1
PD-L2's C-D Latch and W110 Elbow Emerge
N-linked Glycosylation Site
Beta Strand
C
Human Chr. 9
0 Mbp
138 Mbp
4 Mbp
6 Mbp
Human Chr. 9
Chicken Chr. Z
Frog Scaffold GL172722
Coelacanth Scaffold JH127636
JAK2
4.98 Mbp
27.53 Mbp
2.10 Mbp
Scaffold JH128426
PD-L1
5.45 Mbp
27.67 Mbp
2.02 Mbp
0.20 Mbp
PD-L2
5.51 Mbp
27.69 Mbp
1.99 Mbp
RIC1
5.62 Mbp
27.71 Mbp
1.91 Mbp
0.30 Mbp
ERMP1
5.76 Mbp
27.77 Mbp
1.89 Mbp
0.47 Mbp
D
PD-L2's W110 Region
Uniprot# 108-114 V A W D Y K Y
(only has PD-L1)

Figure S3. PD-ligand evolution. (A and B) Phylogenetic analysis of the IgV domains of PD-L2 (A) and PD-L1 (B) . The PD-L2 IgV domain remains highly similar to the primordial PD-L1 sequence from amphibians to marsupial mammals (blue phylogenetic branches). The PD-L2 IgV domain diverged from that of PD-L1 when it acquired an "elbow" and "latch" region upon placental mammal radiation (red phylogenetic branches). (C) Synteny analysis of the PDJ-amplicon of the human 9p24.1 locus (36,37). (D) Phylogenetic DNA sequence analysis of the PD-L2 W110 "elbow." Feline reversion to a Gly codon occurred by a single nucleotide conversion, dissimilar to the Opossum Gly codon.

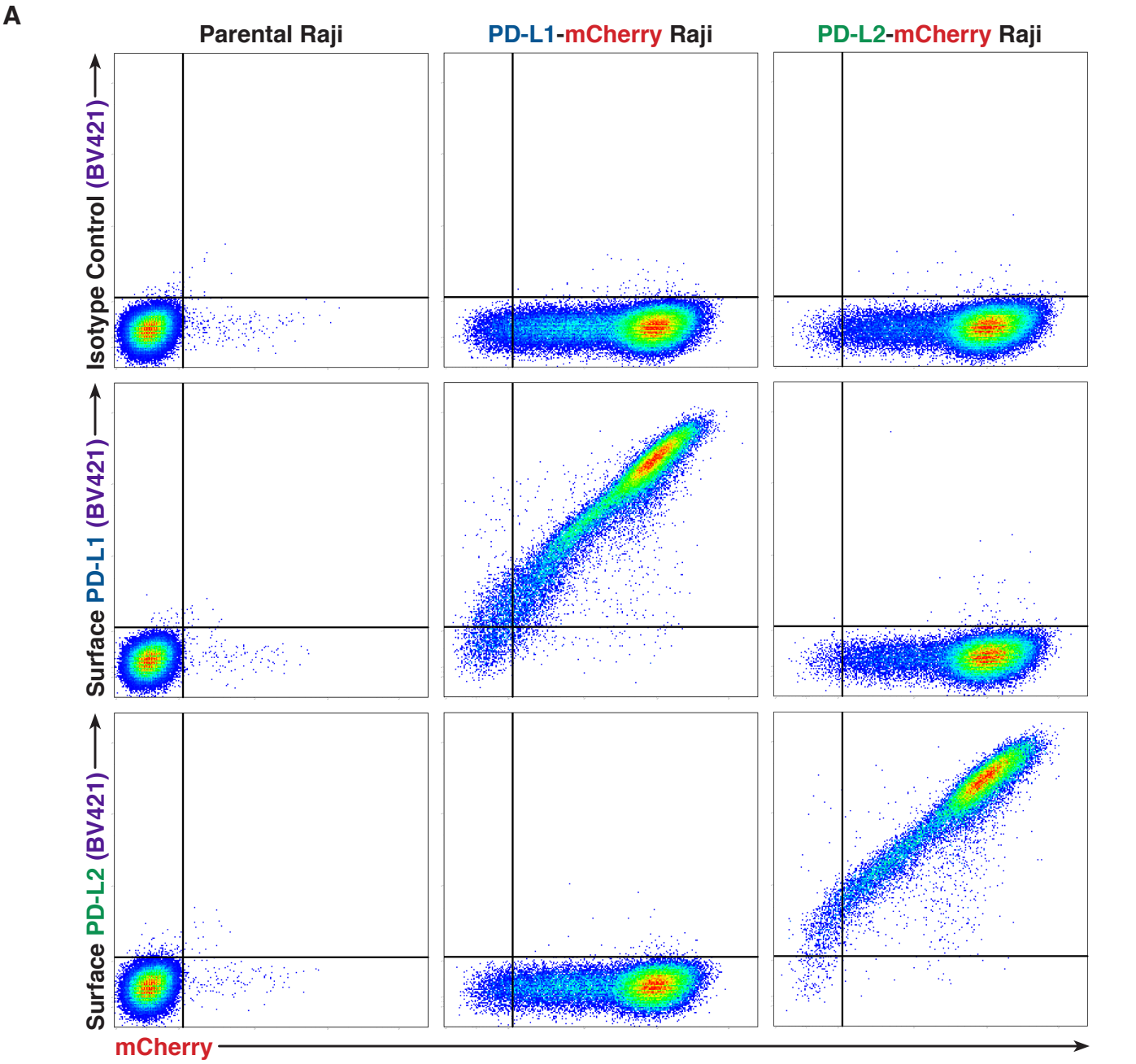
A
Parental Raji
PD-L1-mCherry Raji
PD-L2-mCherry Raji
Isotype Control (BV421)
Surface PD-L1 (BV421)
Surface PD-L2 (BV421)
mCherry

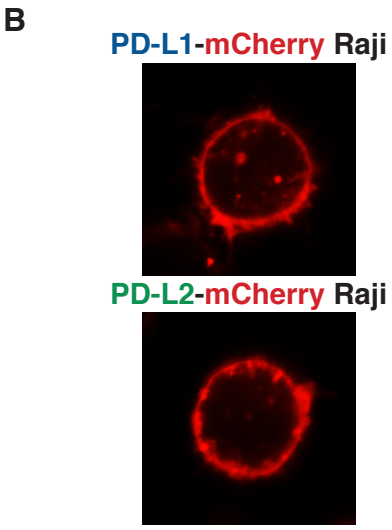
B
PD-L1-mCherry Raji
PD-L2-mCherry Raji

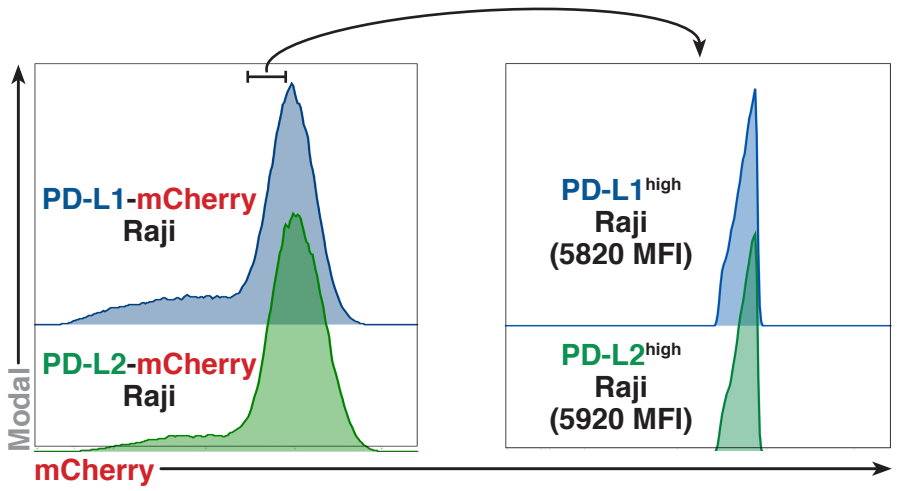
C
PD-L1-mCherry Raji
PD-L2-mCherry Raji
Modal
mCherry
PD-L1high Raji (5820 MFI)
PD-L2high Raji (5920 MFI)

Figure S4. PD-ligandhigh Raji B cell preparation and surface expression validation. (A) Flow cytometry analysis of PD-ligand surface expression for parental, PD-L1-mCherry, and PD-L2-mCherry Raji B cells using BV421 conjugated mAbs. (B) Live cell confocal images of Raji B cells transduced with lentiviruses directing expression of PD-ligand-mCherry. (C) Histogram of PD-ligand-mCherry expression in Raji B cells traduced with lentivirus. Shown is the narrow gate used to assure equivalent expression of each ligand on cells used in primary T cell conjugation assays (Figure 4J).

Common name	Scientific name	DNA sequence	Protein sequence	
		PDL2	PDL2	PDL1
Human	*Homo sapiens*	XM_005251600	XP_005251657	NP_054862.1
Gibbon	*Nomascus leucogenys*	XM_003273827	XP_003273875	XP_003273874
Lemur	*Microcebus murinus*	XM_012737993	XP_012593447	XP_012593388
Mouse	*Mus musculus*	NM_021396	NP_067371	NP_068693
Beaver	*Castor canadensis*	XM_020159594	XP_020015184	XP_020015185
Dog	*Canis lupus familiaris*	XM_022421863	XP_022277571	NP_001278901
Cat	*Felis catus*	-	XP_006939100	XP_006939101
Microbat	*Myotis lucifugus*	XM_014460401	XP_023614190	XP_005861392
Cow	*Bos taurus*	-	XP_024851656	NP_001156884
Dolphin	*Tursiops truncatus*	XM_019934810	XP_019790369	XP_004313647
Tenrec	*Echinops telfairi*	XM_013005646	XP_012861100	XP_012861098
Elephant	*Loxodonta africana*	XM_023545365	XP_023401133 ENSLAFT00000037236	XP_010586356
Armadillo	*Dasypus novemcinctus*	XM_023588443	XP_023444211	XP_023444213
Opossum	*Monodelphis domestica*	XM_007499547	XP_007499609	XP_007499605
Tasmanian Devil	*Sarcophilus harrisii*	XM_012544068	XP_012399522	XP_012399523
Koala	*Phascolarctos cinereus*	XM_021006311	XP_020861970	XP_020861971
Platypus	*Ornithorhynchus anatinus*	XM_007655600	XP_007653790	XP_001506048
Chicken	*Gallus gallus*	XM_004949068	XP_004949125	XP_424811
Duck	*Anas platyrhynchos*	XM_021267840	XP_021123515	XP_012948976
Turtle	*Chrysemys picta bellii*	XM_005296800	XP_005296857	XP_005296856
Crocodile	*Crocodylus porosus*	XM_019555441.	XP_019410986	XP_019410914
Frog	*Xenopus tropicalis*	XM_018090958	XP_01794644	XP_017946448
Coelacanth	*Latimeria chalumnae*	-	-	XP_014349176.1

Supplementary Table 1. Protein and DNA sequence accession numbers.

Supplementary References

35. Abagyan, R., Totrov, M., and Kuznetsov, D. (1994) ICM–A new method for protein modeling and design: applications to docking and structure prediction from distorted native conformation. J. Comput. Chem. 15, 488–506
36. Green, M. R., Monti, S., Rodig, S. J., Juszczynski, P., Currie, T., O'Donnell, E., Chapuy, B., Takeyama, K., Neuberg, D., Golub, T. R., Kutok, J. L., and Shipp, M. A. (2010) Integrative analysis reveals selective 9p24.1 amplification, increased PD-1 ligand expression, and further induction via JAK2 in nodular sclerosing Hodgkin lymphoma and primary mediastinal large Bcell lymphoma. Blood 116, 3268–3277
37. Barrett, M. T., Anderson, K. S., Lenkiewicz, E., Andreozzi, M., Cunliffe, H. E., Klassen, C. L., Dueck, A. C., McCullough, A. E., Reddy, S. K., Ramanathan, R. K., Northfelt, D. W., and Pockaj, B. A. (2015) Genomic aplification of 9p24.1 targeting JAK2, PD-L1, and PD-L2 is enriched in high-risk triple negative breast cancer. Oncotarget. 6, 26483–26493